

# Hybrid Enhancement Technique of Retinal Fundus Image Using Reconstruction Filter Segmentation with Various Classification and Optimization Methods

N.Sathya<sup>1</sup>, P.Suresh<sup>2</sup>, N.Rathika<sup>3</sup>

<sup>1,2,3</sup> Department of Electronics and Communication Engineering, P.S.N. College of Engineering and Technology, Tirunelveli, Tamil Nadu, India.

sathyaie@gmail.com ,sathyanatarajan083@gmail.com, suresh3982@gmail.com, rathika.111287@gmail.com

**Abstract-** Diabetic complication causes variation in the retinal blood vessel, channels to Diabetic Retinopathy (DR) and the retinal blood vessel gets distorted. The exudates are concealed; microaneurysms and hemorrhages arise in the retina. These features represent the disease severity. DR eye disease which is harmful causes pressure in eye nerve fiber. It is essential to diagnose it earlier. The proposed approach is used for the detection of severity of DR. The proposed approach starts with preprocessing using hybrid enhancement technique, reconstruction filter segmentation, extraction of Gabor Features (GF) and Histogram of Oriented Gradients Features (HOGF), classification and optimizations. Publicly available databases such as DRIVE, STARE, MESSIDOR and Real time fundus images are taken for analysis for performance comparison.

**Keywords:** Hybrid Enhancement, Reconstruction Filter Segmentation, Features Extraction, Classifiers, Optimizations.

## 1. Introduction

The fundus is the only organ in the human body which is capable of observing the microcirculation [1] directly, containing the retina, optic disc, macula, fovea, and posterior pole. The light sensitive cells (cones and rods) covered by the retina are liable for fulltime vision. The Figure 1 shows the human eye. The human eye can be divided into outer and inner regions. The outer region of the eye consists of two parts: the anterior cornea, a transparent layer with optical [2] power through which light enters the eye; and the posterior sclera, a dense, white, opaque layer providing a boundary at the rear of the eye. Major structures within the inner eye include the iris, a ring of tissue

which forms the aperture stop of the eye; the lens, providing additional optical power; the ciliary body, a ring of tissue surrounding the lens; and the retina, a layered tissue structure where an optical image of the external world is formed and sensed.

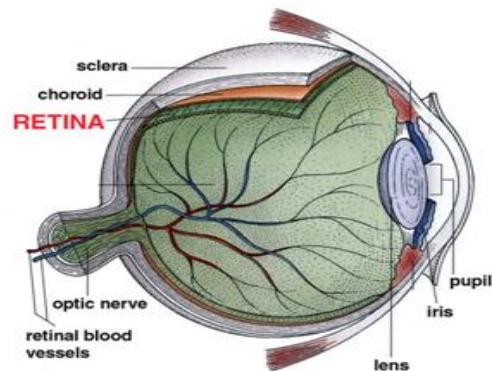
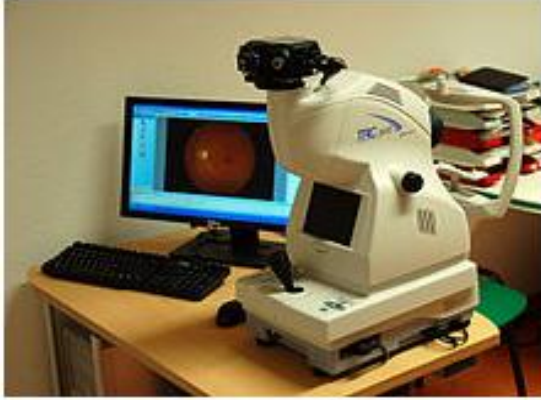


Figure 1. Human eye

The inner region of the eye consists of three parts: the anterior chamber, lying between the cornea and iris and containing aqueous fluid; the posterior chamber, framed by the lens, iris, and ciliary body and containing aqueous fluid; and the vitreous chamber, lying between the lens and retina and containing a gelatinous mass called the vitreous humour. Between the retina and sclera is a blood-rich layer, the choroid, which supports [3] the metabolic processes in the retina. The path of image-forming light through the eye is: cornea, aqueous fluid, lens, vitreous humour, and retina. Retina images captured by fundus camera as shown in the Figure 2.



**Figure 2. Fundus camera**

Diabetic population may suffer from several eye specific problems resulting to severe vision loss or even blindness. Diabetic Retinopathy (DR) is the most common [4] diabetic eye pathology and has two main stages - Non Proliferative Retinopathy (NPR) and Proliferative Retinopathy (PR) as shown in the Figure 3.

The NPR is divided into three stages:

1. Mild NPR: Microaneurysm is the first sign of diabetic retinopathy and it is the early stage of the disease. This lesion corresponds to small areas of balloon-like swelling in the retinal blood vessels. Initially microaneurysms are red, but eventually become yellower over time.
2. Moderate NPR: Increased microaneurysms swelling cause the occlusion of blood vessels.
3. Severe NPR: More blood vessels are blocked which reduces the flow of blood to the retina. So the tissue sends signals to the body, to grow collaterals for the nourishment.

Along with microaneurysms, other lesions may appear during NPR stages, such as hard exudates (yellow extracellular accumulations of [5] lipoproteins resulting from abnormal vessels leakage) and intra retinal haemorrhages (as a result of microaneurysms rupture).

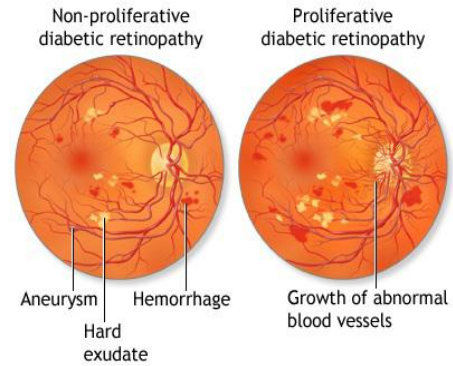


**Figure 3. Types of Diabetic Retinopathy**

Proliferative Retinopathy is the advanced stage. It is a consequence of the body response causes the growth of collaterals during the advanced NPR stage. These new collaterals are abnormal and fragile, fluid leaks into the centre of the macula, it causes [6-8] macula swelling and thickening, blurring vision termed as macular edema. At early stage DR is a treatable pathology.

## 2. Methodology

The process involved in the proposed system: (a) Reads the fundus image, (b) Hybrid Enhancement Preprocessing, (c) Reconstruction Filter Segmentation, (d) Features Extraction (GF, HOGF), (e) Classifiers (Adaboost, DSVM, ELMASR, EPLS, KNN, NB, NBFFS, OCPLS, RBFN, RF, SOWA, SVM, SVNN and NF-SCG), (f) Optimizations (GWO, HPSO, GSA, FO-HPSOGSA, BBO, PSO, GA, ACO, ES and PBIL). These techniques are explained in the following sections. The flow diagram of the proposed system as shown in the Figure 5.

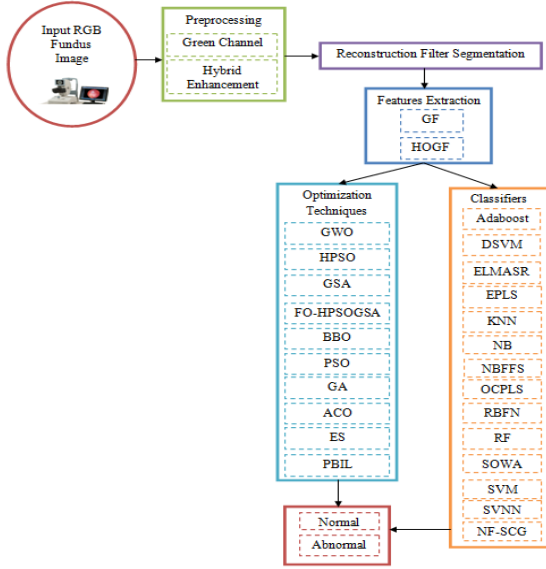


**Figure 5. Flow diagram of the proposed system**

### 3. Performance Measure

By classifying the patients with respect to the test results and the true disease status based on the confusion matrix with nine performance assessments. First eight performance assessments are compared with KNN, NB, NBFSS, DSVM, and SVM classifiers and comparing accuracy (Acc) measurement with all classifiers except OCPLS. OCPLS classifier types are compared with SD and ACR. The performance assessment of the proposed methodology is analyzed with the following parameters using this formula from Equation (1-8).

$$\text{Sensitivity } (Se) = TP / (TP + FN) = TP/nD \quad (1)$$

$$\text{Specificity } (Sp) = TN / (FP + TN) = TN/nC \quad (2)$$

$$\text{Prevalence } (Pr) = (TP + FN) / (TP + FP + FN + TN) = nD/n \quad (3)$$

$$\begin{aligned} \text{Positive Predictive Value } (PPV) &= TP / (TP + FP) \\ &= TP/nP \end{aligned} \quad (4)$$

$$\begin{aligned} \text{Negative Predictive Value } (NPV) &= TN / (TN + FN) = \\ &= TN/nN \end{aligned} \quad (5)$$

$$\text{Likelihood Ratio Positive } (LRP) = Se / (1 - Sp) \quad (6)$$

$$\text{Likelihood Ratio Negative } (LRN) = (1 - Se) / Sp \quad (7)$$

$$\text{Agreement } (Ag) = (TP + TN) / n \quad (8)$$

$$\text{Accuracy } (Acc) = (TP + TN) / (TP + FN + TN + FP) \quad (9)$$

### 4. Results and Discussion

The algorithm has been implemented in MATLAB code, in version R2014. Forty images are selected in random from the DRIVE (Digital Retinal Images for Vessel Extraction) database [9]. From these images 33 are without DR symptoms and remaining with mild DR, separated as training and testing sets with 20 images each. These images are captured using Canon CR5 Non-Mydriatic retinal camera with a resolution of 768\*584 and 45° Field of View (FOV) from 400 diabetic patients from the age of 25-90 years. Example for normal and pathological image from the DRIVE dataset is shown in Figure 6.

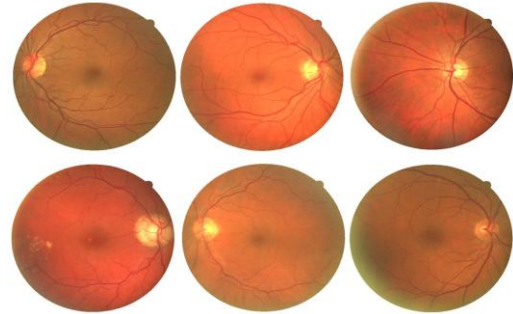


**Figure 6. Different images - DRIVE database**

The STARE (Structured Analysis of Retina) dataset [10] is the oldest and mostly used retinal image database; these images were captured using TopCon TRV-50 retinal camera with 35° FOV. It contains 81 retinal images of which 30 are healthy retinal and 50 are with lesions related to DR. From the STARE dataset a normal and pathological image is shown for example in Figure 7.

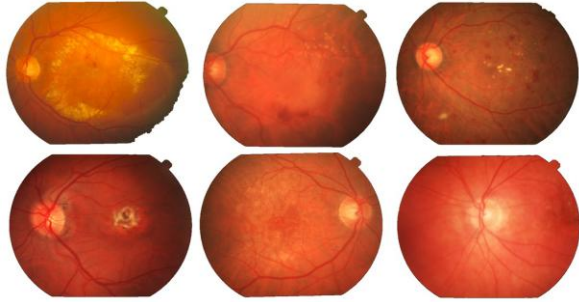


**Figure7. STARE database - Retinal images**

The MESSIDOR (Methods for Evaluating Segmentation and Indexing techniques Dedicated to Retinal Ophthalmology) database [11], facilitates computer aided DR lesions detection. Based on the number and position of lesions, the images are categorized, an example of these images are shown in Figure 8.

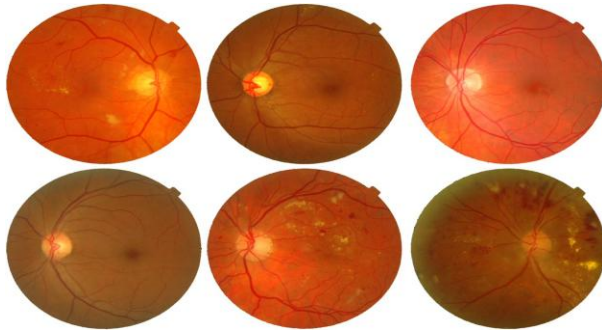


**Figure 8. MESSIDOR database - Retinal images**

The Real time fundus images are taken from Agarwal’s Eye Hospital, Tirunelveli; the images are saved in JPEG format with a size of 1.34 MB per image and resolution of 1916\*1664 pixel. Example of normal and pathological image from the Real Time dataset is shown in Figure 9.

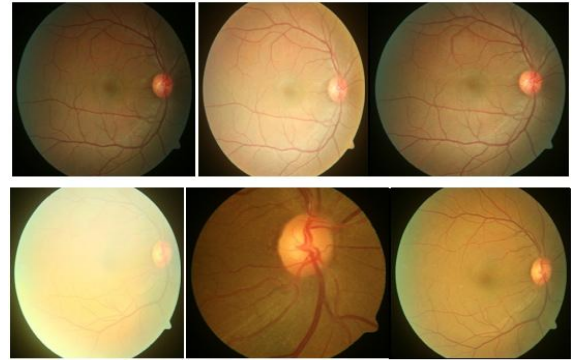


**Figure 9. Different retinal images from Real Time database**

The datasets specified in Table 1 is taken for the evaluation because these dataset images contain varieties of DR lesions which suits well for evaluation. The results are taken from both the dataset which contains both normal and abnormal (i.e contains lesions).

**Table 1. Dataset Specification**

Dataset	Total Images	Training Segment	Testing Segment
DRIVE	40	20	20
STARE	50	20	30
MESSIDOR	90	30	60
Real Time	50	20	30

#### 4.1. Pre-Processing Output

The input image is taken in the RGB form. For pre-processing, first it is converted into green channel and applying hybrid enhancement technique. The Figure 10 shows that the pre-processing output.

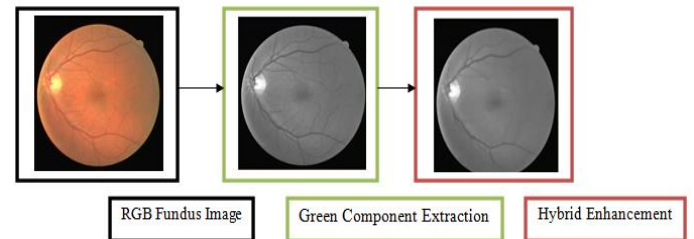


**Figure 10. Pre-processing output**

#### 4.2. Segmentation Output



The Figure 11 shows the segmentation output. After preprocessing, then apply reconstruction filter segmentation technique to segment the blood vessels of enhanced image.



Figure11. Segmentation result

### 4.3. Features Extraction Result

In this section, Gabor Features (GF), Histogram of Oriented Gradients Features (HOGF) of segmented images are extracted. The Table 2 shows that the features extraction result.

Table 2. Features extraction result

Features Extraction	DRIVE	MESSIDOR	STARE	Real Time
GF	2.02E-16	1.19E-16	-1.28E-16	-4.11E-16
HOGF	0.000843	0.000965	0.00083	0.0004

### 4.4. Classifiers and its Performance Outputs

In this section, calculate the performance assessments like Sensitivity (Se), Specificity (Sp), Prevalence (Pr), Positive Predictive Value (PPV), Negative Predictive Value (NPV), Likelihood Ratio Positive (LRP), Likelihood Ratio Negative (LRN), Agreement (Ag), and Accuracy (Acc). The Table 3 shows that the first eight performance assessments on DRIVE, MESSIDOR, Real Time, and STARE databases.

Table 3. Performance assessments on DRIVE, MESSIDOR, Real Time, and STARE databases

Classifiers	Se	Sp	Pr	PPV	NPV	LRP	LRN	Ag
KNN	0.7000	0.6000	0.5000	0.6364	0.6667	1.7500	0.5000	0.6500
NB	0.6667	0.6000	0.3750	0.5000	0.7500	1.6667	0.5556	0.6250
NBFFS	0.6667	0.6000	0.3750	0.5000	0.7500	1.6667	0.5556	0.6250
DSVM	0.5833	0.6250	0.6000	0.7000	0.5000	1.5556	0.6667	0.6000
SVM	0.7500	0.7500	0.5000	0.7500	0.7500	3.0000	0.3333	0.7500

Classifiers	Se	Sp	Pr	PPV	NPV	LRP	LRN	Ag
KNN	0.6522	0.6818	0.5111	0.6818	0.6522	2.0497	0.5101	0.6667
NB	0.6667	0.8333	0.6667	0.8889	0.5556	4.0000	0.4000	0.7222
NBFFS	0.4444	0.4444	0.5000	0.4444	0.4444	0.8000	1.2500	0.4444
DSVM	0.8333	0.6429	0.3000	0.5000	0.9000	2.3333	0.2593	0.7000
SVM	0.8571	0.7273	0.3889	0.6667	0.8889	3.1429	0.1964	0.7778

Classifiers	Se	Sp	Pr	PPV	NPV	LRP	LRN	Ag
KNN	0.4667	0.8000	0.6000	0.7778	0.5000	2.3333	0.6667	0.6000
NB	0.4000	0.4000	0.5000	0.4000	0.4000	0.6667	1.5000	0.4000
NBFFS	0.6000	0.6000	0.5000	0.6000	0.6000	1.5000	0.6667	0.6000
DSVM	0.5000	0.5000	0.1000	0.1000	0.9000	1.0000	1.0000	0.5000
SVM	0.6667	0.7500	0.6000	0.8000	0.6000	2.6667	0.4444	0.7000

Classifiers	Se	Sp	Pr	PPV	NPV	LRP	LRN	Ag
KNN	0.6000	0.8000	0.6000	0.8182	0.5714	3.0000	0.5000	0.6800
NB	0.6667	0.7500	0.6000	0.8000	0.6000	2.6667	0.4444	0.7000
NBFFS	0.4000	0.4000	0.5000	0.4000	0.4000	0.6667	1.5000	0.4000
DSVM	0.3333	0.4286	0.3000	0.2000	0.6000	0.5833	1.5556	0.4000
SVM	0.5000	0.5000	0.6000	0.6000	0.4000	1.0000	1.0000	0.5000

The Table 4 shows that the classification rate (Acc) with different classifiers.

Table 4. Classification rate (Acc) with different classifiers

Classifiers	Ada boost	DSVM	ELM ASR	EPLS	KNN	NB	NBFFS	RBFN	RF	SVM	NF-SCG	SVNN
DRIVE	35	60	50	39	65	63	75	98	66	75	90	100
MESSIDOR	45	70	51	65	67	72	65	100	66	78	97	100
Real Time	35	50	52	37	60	50	68	98	60	70	90	100
STARE	35	40	52	59	68	70	60	98	70	50	96	100

SOWA Classifiers	Basic RIM Acc	Quadratic Acc	Exponential Acc	Trigonometric Acc	O'Hagans Acc
DRIVE	75	75	75	70	75
MESSIDOR	65	63	67	67	63
Real Time	77	80	77	77	70
STARE	60	73	60	60	57

The Table 5 shows that the values of SD and ACR with two types of OCPLS classifier.

Table 5. Values of SD and ACR with two types of OCPLS classifier

Ordinary Linear OCPLS Classifiers	SD	ACR	Non Linear RBF OCPLS Classifiers	SD	ACR
DRIVE	11.2545	1.3203	DRIVE	19.2936	0.0148
MESSIDOR	9.8569	1.0159	MESSIDOR	15.6006	0.0098
Real Time	11.2545	1.1593	Real Time	19.2936	0.0143
STARE	11.2545	1.6650	STARE	19.2936	0.0154

#### 4.5. Optimizations and its Performance Outputs

In this section, calculate the classification rate (Acc) performance assessment is compared and analyzed on all optimization techniques. The Table 6 shows that the Classification rate (Acc) with different optimization techniques.

**Table 6. Classification rate (Acc) with different optimization techniques**

Optimization Techniques	GWO	GSA	HPSO	FO-HPSOGSA	BBO	PSO	GA	ACO	ES	PBIL
DRIVE	50	70	70	70	0	5	0	0	5	0
MESSIDOR	50	61	62	63	0	0	0	0	1.1	4.4
Real Time	50	66	66	66	2	2	0	0	4	2
STARE	50	52	60	60	2	2	0	2	2	0

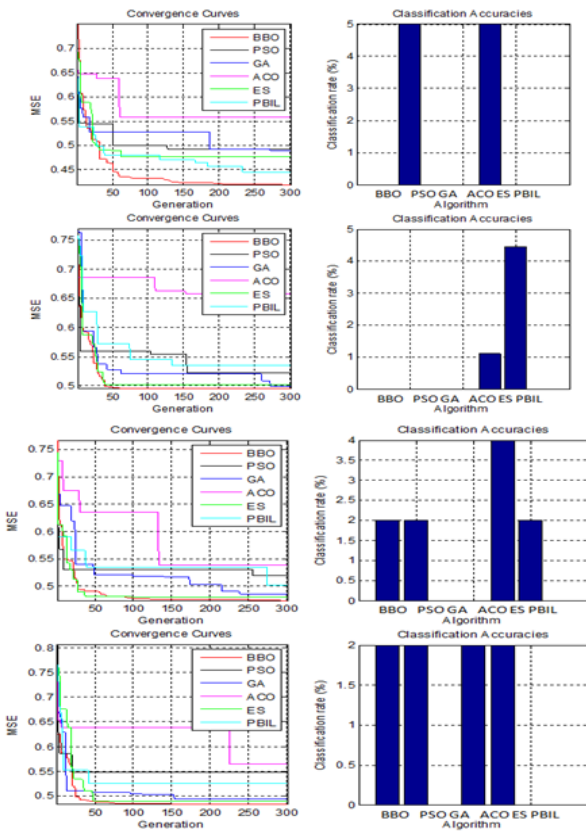


**Figure 12. Graphical representation of performance of the optimizations BBO, PSO, GA, ACO, ES and PBIL**

The Figure 12 shows that the graphical representation of performance of the optimizations BBO, PSO, GA, ACO, ES and PBIL. The following Figure 48 plots the convergence curves and

classification accuracies compared with last six optimization techniques.

#### 5. Conclusion

The proposed system has been developed by applying effective techniques on the fundus images obtained from various databases such as DRIVE, STARE, MESSIDOR and Real Time fundus images taken from Agarwal’s Eye Hospital, Tirunelveli for the diagnosis of Diabetic Retinopathy (DR). By using MATLAB, first enhanced the fundus image using hybrid, segment the blood vessel using reconstruction filter, extracted the features such as GF and HOGF and detected both a normal and a pathological image by applying the classification and optimization techniques. In classification, two types of OCPLS classifier performance is compared with SD and ACR values. Form that results ordinary linear RBF OCPLS has better SD and high ACR values compared with non linear RBF OCPLS. Finally, the performance assessments of all these classifiers (except OCPLS) has been analyzed and compared. From that result, SVNN classifier gives better classification rate when compared with all these classifiers. In optimization, the performance assessments of all these optimization techniques has been analyzed and compared. From that result, FO-HPSOGSA optimization gives better classification when compared with all these optimizations. The proposed system helps the ophthalmologists in the screening process for detecting the symptoms of DR quickly and more easily. This can be used as a preliminary diagnosis tool or decision support system for ophthalmologists.

#### References

- [1] E.J. Susman, W.J. Tsiaras, and K.A. Soper, “Diagnosis of Diabetic Eye Disease”, JAMA. Vol.247,pp. 3231- 3234,1982.
- [2] R. Phillips, J. Forrester, and P. Sharp, “Automated Detection and Quantification of Retinal Exudates”. Graefes Arch. Clin. Exp. Ophthalmol. Vol.231,pp.90-94,1993.
- [3] J. Kansky, Clinical Ophthalmology. London: Butterworth-Heinmann. 1994.
- [4] R. Klein, Diabetic retinopathy, Public Health, vol. 17, pp. 137–158, May 1996.

- [5] A. Pinz, S. Bernogger, P. Datlinger, and A. Kruger, "Mapping the Human Retina". IEEE Trans. Med. Imag., Vol.17, No.4,pp. 606-619,1998.
- [6] A. Sinthanayothin, JF. Boyce, HL. Cook, TH. Williamson, "Automated Localization of the Optic Disc. Fovea and Retinal Blood Vessels from Digital Color Fundus Images". Br. J. Ophthalmol., Vol. 83,pp. 231-238,1998.
- [7] SC. Lee, ET. Lee, RM. Kingsley, YWang, D Russell, R Klein, and A. Wanr, "Comparison of Diagnosis of Early Retinal Lesions of Diabetic Retinopathy between a Computer System and Human Experts",Graefes Arch. Clin. Exp. Ophthalmol. Vol.119,pp. 509-515,2001.
- [8] T. Teng, M. Lefley, and D. Claremont, "Progress towards Automated Diabetic Ocular Screening: A Review of Image Analysis and Intelligent Systems for Diabetic Retinopathy", Med. Biol. Eng. Comput. Vol.40,pp. 2-13,2002.
- [9] P. Perona, and J. Malik, "Scale-space and edge detection using anisotropic diffusion", IEEE Trans. Pattern Anal. Mach. Intel., Vol.12,pp. 629-639,1990.
- [10] DRIVE: Digital Retinal Images for Vessel Extraction,<http://www.isi.uu.nl/Research/Databases/DRIVE/>, 2004.
- [11] STARE: STructured Analysis of the Retina,<http://www.isi.uu.nl/Research/Databases/STARE/>, 2004.
- [12] MESSIDOR: Methods for Evaluating Segmentation and Indexing techniques Dedicated to Retinal Ophthalmology, <http://www.isi.uu.nl/Research/Databases/MESSIDOR/>, 2005.